A Direction Space Interpolation Technique for Calibration of Electromagnetic Surgical Navigation Systems

Xiaohui Wu and Russell Taylor

Engineering Research Center for Computer Integrated Surgical Systems and Technology,
Department of Computer Science, Johns Hopkins University,
Baltimore, MD 21218, USA
{xiaohui.wu, rht}@ jhu.edu

Abstract. A new generation of electromagnetic (EM) navigation systems with extremely compact sensors have great potential for clinical applications requiring that surgical devices be tracked within a patient's body. However, electromagnetic field distortions limit the accuracy of such devices. Further, the errors may be sensitive both to position and orientation of EM sensors within the field. This paper presents a computationally efficient method for *in-situ* 5 DOF calibration of the basic sensors of a typical EM system (Northern Digital's Aurora), and presents preliminary results demonstrating an improvement of approximately 2.6 : 1 positional accuracy and 1.6 : 1 for orientation even when the sensors are moved through arbitrary orientation changes. This work represents one step in a larger effort to understand the field distortions associated with these systems and to develop effective and predictable calibration and registration strategies for their use in stereotactic image-guided interventions.

1 Introduction

Localization devices are critical components in image-guided surgery. A number of technologies have been used for this purpose, including encoded mechanical linkages, acoustic sensors, specialized optical devices, conventional video triangulation, and electromagnetic devices. Currently, specialized optical devices such as Northern Digital's Optotrak ® are generally the most accurate and least affected by environmental disturbances in the operating room (OR), but have several limitations. In particular, the necessity of maintaining a direct line of sight between optical markers and the sensing system can complicate OR logistics and makes direct sensing of positions inside the patient's body impossible. Electromagnetic (EM) sensors avoid these difficulties, but have traditionally been too large for intracorporeal use, and their accuracy is adversely affected by electromagnetic field disturbances. A new generation of EM trackers, such as Johnson & Johnson's Biosense [1] and Northern Digital's Aurora™ systems have very small sensors suitable for use inside catheters and surgical instruments. The Aurora sensors shown in Figure 1 are 8 0.8 ×mm, and their use has been

R.E. Ellis and T.M. Peters (Eds.): MICCAI 2003, LNCS 2879, pp. 215–222, 2003.

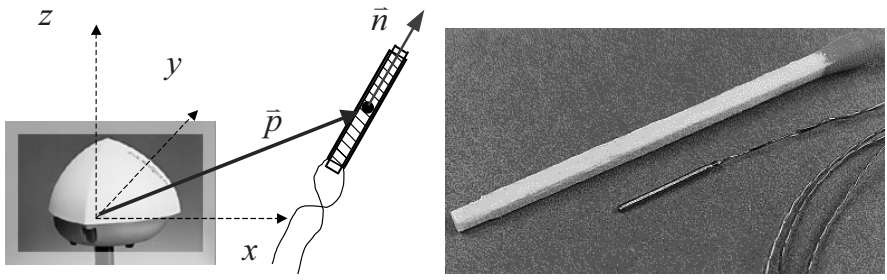

Fig. 1. Aurora field generator (left), 5D sensor (right) and measurement ($\vec{n}$, $\vec{p}$) (center)

explored for a variety of applications including as spine surgery [2], respiratory [3], biopsy needle tracking etc. as well as conventional intravascular use. Pairs of 5DOF sensors have also been combined to make very compact 6DOF sensors (Traxtal Inc.). However, inaccuracy due to electromagnetic field distortion is still an important limitation. Generally, the repeatability of these devices is much better than their absolute accuracy, so it is useful to consider methods for characterizing the field distortion in a particular environment and using the results to improve geometric accuracy. Glossop, et al. [4] evaluated the accuracy of an early version of the Aurora and reported position repeatability 0.2 mm and accuracy of 1.7 mm RMS error.

In earlier work [5], we have reported a method for cross-calibration of 6DOF Aurora sensors against an Optotrak optical navigation system. In this study, we constructed a calibration object containing both Optotrak LED markers and Traxtal 6DOF Aurora markers and attached additional LED markers to the Aurora field generation. We used a small plastic robot to move the calibration object in various orientations through the work volume and constructed polynomial models for the error function.

Although in most of the past research work on various types of magnetic tracker calibration reported that both the position and orientation components of the error was the function the tracked sensor position only [6]. In our previous study, we found this assumption didn't hold for Aurora, when the sensor remains the same orientation, both the position and orientation errors can be corrected by around 90%. However, many practical applications require that the sensor be reoriented unpredictably within the surgical field.

Unfortunately, straightforward extension of techniques that work well in 3 DOF position space to 5 or 6 DOF position + orientation space can become rather cumbersome because of the amount of data that must be gathered. In this paper, we make the simplifying assumption that the geometric errors associated with different sensor orientations can be calibrated *independently* and then combined by interpolation. The resulting method is illustrated for 5 DOF Aurora sensors, but is readily extended to 6 DOF. In subsequent sections, we will first describe our experimental setup and pro-

cedure for producing 5 DOF error maps $E_j(\vec{p})$ over the Aurora workspace for different sensor orientations $\vec{n}_j$. We will then describe a simple scheme for interpolating between orientations and will present preliminary experimental results.

2 Aurora Measurement and Error Representation

The "raw" 5DOF Aurora sensors (Fig. 1) consist of a small coils wound around 0.8mm×8mm iron cores. They are packaged into various end-used devices such as catheters and biopsy devices. The Aurora system essentially determines the position $\vec{p}$ of the center of the sensor, together with the direction $\vec{n}$ of the core. For any set of 5D measurements $M_i = (\vec{p}_i, \vec{n}_i)$, we assume that the corresponding "true" values are a given by $M_i^* = (p_i^*, n_i^*)$. We define the error associated with M_i as

$$E_i = M_i - M_i^* = \left(R^{err}{}_i, \ \vec{\varepsilon}_i\right) \approx \left(\vec{\rho}_i, \ \vec{\varepsilon}_i\right) \tag{1}$$

where we represent the error as a pair

$$\vec{\rho}_i = \vec{n}_i^* \times \vec{n}_i \qquad \vec{\varepsilon}_i = \vec{p}_i - \vec{p}_i^* \tag{2}$$

so that the rotation that transforms $\vec{n}_i^*$ into $\vec{n}_i$ is given by

$$R_i^{err} \approx Rot(\vec{\rho}_i, \sin^{-1} \| \vec{\rho}_i \|) \tag{3}$$

We use this form to represent orientation error because it is straightforward and has no singularity problem.

3 Calibration Apparatus and Experimental Setup

Our experimental setup is shown in Fig. 2. Same as in our earlier study [6], we use an Optotrak 3020 as our calibration standard. Optotrak LED markers were also placed

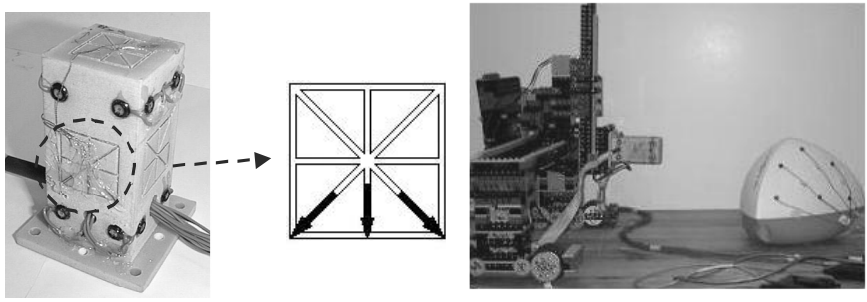

Fig. 2. Aurora Calibration Object (left), Groove pattern on the surface of the fixture (center, black arrows represent the sensors), and the plastic robot with the Aurora field generator.

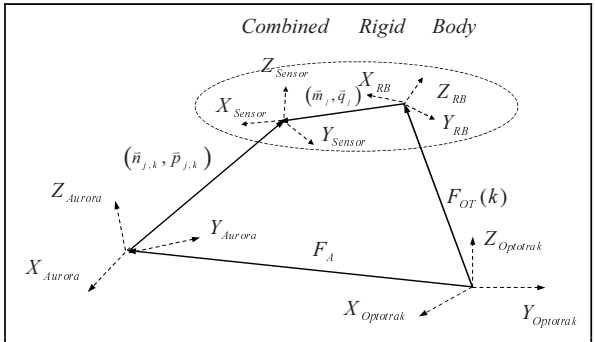

Fig. 3. Registration of Optotrak and Aurora coordinates. The goal is to determine F_A

on the Aurora field generator and used to define a "rigid body" base coordinate system for these experiments. Except where otherwise stated, all Optotrak measurements described in this paper are expressed relative to this coordinate system rather than with respect to the camera.

Our calibration object (Fig. 2, left & middle) consists of a rectangular plastic block with a pattern of grooves machined into each face. 16 Optotrak LED markers were epoxied to the faces of the block and used to define a "rigid body" whose pose F_{OT} with respect to the field generator LEDs could be determined by the Optotrak system. An instrumented Optotrak pointer was used to determine the line equations of each groove with respect to F_{OT} and eight 5 DOF Aurora sensors were embedded into a subset of the grooves, distributed so as to minimize interference between sensors. The sensors were placed into corner points so that line intersections could be used to estimate the position of the sensors. The calibration object could either be mounted on a small plastic LEGO® robot or held freehand to position it within the Aurora workspace.

4 Registration of Aurora Coordinates to Optotrak Coordinates

Fig. 3 shows the relationship between different coordinate systems. Our goal is to determine the unknown transformation F_A between Optotrak and Aurora coordinates. $F_{OT}(k)$ is the Optotrak pose of the calibration object in the k^{th} data acquisition cycle, $(\vec{n}_{j,k}, \vec{p}_{j,k})$ is the j^{th} Aurora sensor measurement in the k^{th} data acquisition cycle. $(\vec{m}_j, \vec{q}_j)$ is the position and orientation of the j^{th} Aurora sensor relative to the Optotrak rigid body, which is characterized using the method described in Section 3. The key relationships are:

$$R_A \vec{n}_{j,k} = R_{OT}(k)\vec{m}_j \tag{4}$$

$$F_A \vec{p}_{j,k} = F_{OT}(k)(\vec{q}_j + \zeta_j \vec{m}_j) \tag{5}$$

where the ζ_j are small displacements to account for the fact that it is difficult to place the sensors exactly at the ends of grooves. The rotation component of R_A can be determined using equation (4) with Horn's quaternion point cloud registration method in [7]. The translation component $\vec{p}_A$ and correction factors ζ_j can then be determined using equation (5) using least squares estimation.

5 Calibration Procedure

Spatial calibration is performed as follows. The calibration object is affixed rigidly to our 3 DOF plastic robot, which translates it to N_{run} positions in the workspace. At each position k, we record a "data frame" $\{F_{OT}(k),(\vec{p}_{1,k},\vec{n}_{1,k}),...,(\vec{p}_{8,k},\vec{n}_{8,k})\}$. The values of $\vec{n}_{j,k}$ are averaged[1] to produce a set of direction basis vectors $\vec{d}_j$

$$\vec{d}_j = \left(\sum\nolimits_k \vec{n}_{j,k}\right) \Big/ N_{run} \tag{6}$$

This process may be repeated multiple times with the calibration object affixed to the robot in different poses to increase the number of $\vec{d}_j$. We compute F_A and update $\vec{q}_j \leftarrow \vec{q}_j + \zeta_j \vec{m}_j$ using the method described in Section 4. Then, we estimate the "ground truth" values for 5 DOF pose from

$$\begin{aligned} \vec{p}_{j,k}{}^{*} &= F_A^{-1} \cdot F_{OT}(k) \cdot \vec{q}_{j,k} \\ \vec{n}^{*}_{j,k} &= R_A^{-1} \cdot R_{OT}(k) \cdot \vec{m}_{j,k} \end{aligned} \tag{7}$$

and compute $E_{j,k}$ from (1)-(3).

For each Aurora direction basis $\vec{d}_j$, obtain the characterized error functions $E_j(\vec{p}) = (\vec{\rho}_j, \vec{\varepsilon}_j)(\vec{p})$. Typically, we represent $E_j(\vec{p})$ either as a multivariable Bernstein polynomial of moderately high degree (3-5) or as a k-d tree of polynomials of lower degree (0-1). Detailed description of the method can be found in [4].

6 The Orientation Interpolation Technique

Suppose that we are given a spherical triangle $(\vec{a},\ \vec{b},\ \vec{c})$, with $\|\vec{a}\| = \|\vec{b}\| = \|\vec{c}\| = 1$. We have another point $\vec{v}$ inside the triangle, with $\|\vec{v}\| = 1$. want to find three weights $(\alpha,\ \beta,\ \gamma)$ with $\alpha + \beta + \gamma = 1$ associated with $\vec{v}$ that we can use to interpolate errors associated with the vertices $\vec{a},\ \vec{b},\ \vec{c}$. I.e., if the errors associated with three direction vectors $\vec{a},\ \vec{b},\ \vec{c}$ defining a spherical triangle containing $\vec{v}$ are E_a, E_b, E_c, we want to find weights so that we approximate the error at $\vec{v}$ as

$$E_v = \alpha E_a + \beta E_b + \gamma E_c \tag{8}$$

We define a function

$$ArcInterpolate(\lambda, \vec{a}, \vec{b}) = Rot\left(\vec{a} \times \vec{b},\ \ \lambda \sin^{-1} \left\|\vec{a} \times \vec{b}\right\|\right) \bullet \vec{a} \tag{9}$$

---

[1] This averaging step is based on the assumption that the robot provides only purely translational motion. It is neither strictly accurate nor necessary, but it does simplify the procedure and explanation without introducing significant error.

to interpolate a point a fraction λ of the way along the circular arc from $\vec{a}$ to $\vec{b}$. Analogous to the case of planar triangle, we can compute weights, $0 \le \lambda, \mu \le 1$ such that

$$\vec{v} = ArcInterpolate\left(ArcInterpolate\left(\mu, \vec{c}, ArcInterpolate\left(\lambda, \vec{a}, \vec{b}\right)\right)\right) \tag{10}$$

Then we compute

$$\alpha = \mu - \lambda\mu \quad \beta = \lambda\mu \quad \gamma = 1 - \mu \tag{11}$$

to obtain the desired weights. For more general vectors, we define

$$ArcInterpolate\left(\lambda, \vec{a}, \vec{b}\right) = \left((1-\lambda)\left\|\vec{a}\right\| + \lambda\left\|\vec{b}\right\|\right) ArcInterpolate\left(\lambda, \frac{\vec{a}}{\left\|\vec{a}\right\|}, \frac{\vec{b}}{\left\|\vec{b}\right\|}\right) \tag{12}$$

To solve for λ and μ, we first compute a rotation **R** such that

$$R \bullet \left(\vec{a} \mid \vec{b} \mid \vec{c}\right) = \begin{pmatrix} 1 & \cos\theta & q_x \\ 0 & \sin\theta & q_y \\ 0 & 0 & q_z \end{pmatrix} \tag{13}$$

We solve $R \bullet \vec{b} = [\cos\theta,\ \sin\theta,\ 0]^T$ for θ, and then compute

$$\vec{q} = R \bullet \vec{c} \qquad \vec{u} = R \bullet \vec{v} \qquad \vec{n} = \vec{q} \times \vec{u} = \vec{q} = R \bullet \left(\vec{c} \times \vec{v}\right) \tag{14}$$

If $\left\|\vec{n}\right\| = 0$, take $\mu = 0,\ \lambda = arbitrary$. Otherwise, find the point $\vec{s} = [\cos\sigma,\ \sin\sigma,\ 0]^T$ on the arc $\left(\mathrm{R} \bullet \vec{a}, R \bullet \vec{b}\right)$ that intersects the plane $\vec{n} \bullet \vec{s} = 0$.

$$\vec{n} \bullet \vec{s} = n_x \cos\sigma + n_y \sin\sigma = 0 \tag{15}$$

We pick a solution for σ such that $0 \le \sigma \le \theta$. Then compute

$$\lambda = \frac{\sigma}{\theta} \quad \mu = \frac{\sin^{-1}\left\|\vec{q} \times \vec{u}\right\|}{\sin^{-1}\left\|\vec{q} \times \vec{s}\right\|} \tag{16}$$

and compute $(\alpha,\ \beta,\ \gamma)$ using equation (11).

7 Error Correction Procedure and Validation Tests

For validation, we removed the calibration object from the robot and placed it manually in a number of different poses with respect to the Aurora field generation unit, and gathered data frames $\{F_{OT}(k), (\vec{p}_{1,k}, \vec{n}_{1,k}), ..., (\vec{p}_{8,k}, \vec{n}_{8,k})\}$ for each pose k. For each Aurora measurement $M_{j,k} = (\vec{p}_{j,k}, \vec{n}_{j,k})$ we find the spherical triangle $\left(\vec{d}_a, \vec{d}_b, \vec{d}_c\right)$ encompassing $\vec{n}_{j,k}$. We then compute weights $(\alpha,\ \beta,\ \gamma)$ as in Section 6 and interpolate

$$E_{j,k}(\vec{p}_{j,k}) = (\vec{\rho}_{j,k}, \vec{\varepsilon}_{j,k}) = \alpha E_a(\vec{p}_{j,k}) + \beta E_b(\vec{p}_{j,k}) + \gamma E_c(\vec{p}_{j,k}) \tag{17}$$

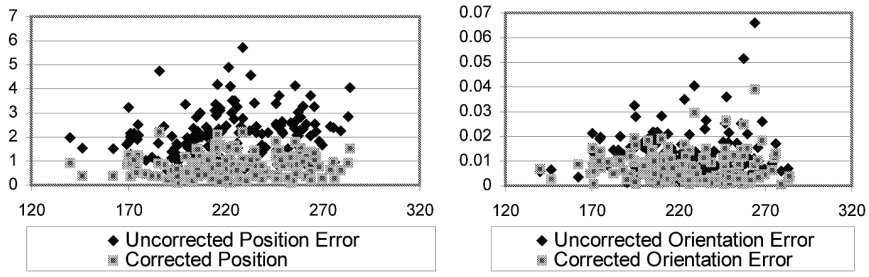

Fig. 4. Position and orientation error vector length as function of x coordinate (mm) of Aurora. Unit for position error is mm; unit for orientation error is radians

We then estimated $M_{j,k}^{*}$ from

$$\vec{n}_{j,k}^{*} = Rot(\vec{\rho}_{j,k}, -\|\vec{\rho}_{j,k}\|) \bullet \vec{n}_{j,k} \qquad \vec{p}_{j,k}^{*} = \vec{p}_{j,k} - \vec{\varepsilon}_{j,k} \tag{18}$$

and compared these values with those obtained (4) and (5).

8 Results and Discussion

For the experiment, we calibrated a cube with volume size of around $(200\text{mm})^3$ in front of the Aurora field generator. During the data acquisition process, the fixture was oriented in four poses, and a total of 24 direction bases data were acquired. 6 direction bases are along the positive as well as negative axes of the Cartesian coordinate system. 12 direction bases are in the Cartesian planes and along the line dividing two neighboring axes, the other direction basis are pointing to random directions away from all the above bases. For each direction basis, roughly 1000-1500 measurements are acquired within the volume. In the verification stage, a total 179 poses were acquired. Since it is impractical to cover both the position and orientation space in this stage, we place more emphasis on the variation of orientation to study the effective-ness of our orientation interpolation method. Procedures are followed as described in Section 6. Table 1 shows the comparison of average error length before correction and after correction, which are computed as described in section 6. In both cases, 4th order Bernstein polynomials were to construct the error approximation.

Table 1. Position and Orientation error vector length before correction and after correction

		before correction	after correction	Improvement
Arbitrary poses	Position (mm)	2.05	0.80	2.6 : 1
	Orientation (rad)	0.013	0.0079	1.6 : 1
Fixed poses	Position (mm)	1.42	0.34	4.2 : 1
	Orientation (rad)	0.011	0.0045	2.4 : 1

We have presented a framework for calibrating a magnetic tracking device using a more accurate tracker. In particular we addressed the pose dependence of the tracking error. Note this experiment was performed in a setup while field distorting sources such as computers, printers and surgical robots etc are close by. The results show that Aurora magnetic tracker may be well suited for medical application, a natural extension of this work would be to carry out the same experiment in the operating room, characterize and further correct the distorting effects of common surgical equipments and devices. Additionally we are also interested in using this system in tracking an ultrasound probe and reconstruct 2D images in 3D space.

Acknowledgements. This work was funded in part by Northern Digital, Inc., under research support provided to the CISST ERC. We are most grateful for this support and for the collaboration of Saibal Chakraburtty, Jeff Stanley, Anton Deguet and Anand Viswanathan, who provided helpful software, equipment, and consultation support.

References

1. http://www.biosensewebster.com
2. K. R. Cleary, M. Clifford, D. Stoianovici, M. Freedman, S.K. Mun, V. Watson: Technology improvements for image-guided and minimally invasive spine procedures. In: IEEE Transactions on Information Technology in Biomedicine, Vol. 6 No. 4 , pp. 249–261, 2002.
3. K. R. Cleary, F. Banovac, E. Levy, D. Tanaka: Development of a liver respiratory motion simulator to investigate magnetic tracking for abdominal interventions. In: Proc. SPIE Vol. 4681, pp. 25–29, 2002.
4. N. Glossop, F. Banovac, E. Levy, D. Lindisch, and K. Cleary: Accuracy Evaluation of the AURORA Magnetic Tracking System, Presented at CARS 2001 (Computer Assisted Radiology and Surgery), 15th International Congress and Exhibition , June 27–30, 2001 ICC Berlin, Germany
5. X. Wu, R. H. Taylor: A Framework for Calibration of Electromagnetic Surgical Navigation System. Submitted to: International Conference on Intelligent Robots and Systems, Las Vegas, USA, 2003
6. V. Kindratenko: A Survey of Electromagnetic position tracker calibration techniques. In: Virtual Reality: Research, Development, and Applications, vol. 5, no. 3, pp.169–182, 2000.
7. B.K.P. Horn: Closed form solution of absolute orientation using unit quaternions. In: J. Opt. Soc. America, A vol. 4, no. 4, pp 629–642, Apr. 1987.
8. http://www.ndigital.com. Northern Digital Product Information